Available online at www.sciencedirect.com
SCIENCE DIRECT®
Physica E 16 (2003) 17–23
PHYSICA E
www.elsevier.com/locate/physe

Electronic memory effects in self-assembled monolayer systems

J. Chen, J. Su, W. Wang, M.A. Reed*

Departments of Electrical Engineering, Applied Physics, and Physics, Yale University, P.O. Box 208284, New Haven, CT 06520, USA

Abstract

We report stable and reproducible switching and memory effects in Self-Assembled Monolayers (SAMs). We demonstrate realization of negative differential resistance (NDR) and charge storage in electronic devices that utilize single redox-center-contained SAM as the active component; and compare the effects of various redox centers to switching and storage behavior. The devices exhibit electronically programmable and erasable memory bits with bit retention times greater than 15 min at room temperature.
© 2002 Elsevier Science B.V. All rights reserved.

Keywords: Self-assembled monolayer; Molecular transport

Electronic switching and memory effects are known to exist in a wide variety of inorganic and organic materials. In 1979, Potember et al. [1] reported bistable, reproducible, and nanosecond electronic switching and memory phenomena in an organometallic charge-transfer (CT) complex salt CuTCNQ formed by TCNQ (7, 7, 8, 8-tetracyano-*p*-quinodimethane), which acts as an electron acceptor with metallic copper as the electron-rich donor. In these materials the switching and memory phenomena are given rise to by the field assisted structural changes such as phase transitions, crystallization, and metal filament formation assisted by highly localized Joule heating. However, the electronic behavior of these materials is mostly not stable or reproducible, and usually requires high switching voltage [2].

In this paper we discuss stable and reproducible switching and memory effects in self-assembled monolayer (SAMs). We first present results on stable and reproducible large negative differential resistance (NDR) and charge storage in electronic devices that utilize single redox-center-contained SAM as the active component. The devices exhibit electronically programmable and erasable memory bits with bit retention times greater than 15 min at room temperature.

A molecule containing a nitroamine redox center (2′-amino-4, 4′-di(ethynylphenyl)-5′-nitro-1-benzenethiolate) is used in the active SAM. Its structure is illustrated in Fig. 1. Apart from the ethynylphenyl based backbone, there is a redox center introduced in the middle benzene ring: the electron withdrawing nitro ($-NO_2$) group and the electron rich amino ($-NH_2$) group.

To deposit the SAM layer onto gold electrode, we transfer the prefabricated nanopores into a 0.5 mM 2′-amino-4, 4′-di(ethynylphenyl)-5′-nitro-1-(thioacetyl)benzene (**1a**) in THF solution. The thioacetyl groups are then selectively hydrolyzed with ammonium hydroxide (concentrated aqueous 14.8 M NH_4OH, 5 μl/mg of **1a**) in tetrahydrofuran (THF) to yield the free thiol, 2′-amino-4, 4′-di(ethynylphenyl) -5′-nitro-1-benzenethiol (**1b**), which then forms the thiolate, 2′-amino-4, 4′-(diethynylphenyl)-5′-nitro-1-

* Corresponding author. Fax: +1-203-432-6420.
E-mail address: mark.reed@yale.edu (M.A. Reed).

1386-9477/02/$ - see front matter © 2002 Elsevier Science B.V. All rights reserved.
PII: S1386-9477(02)00577-5

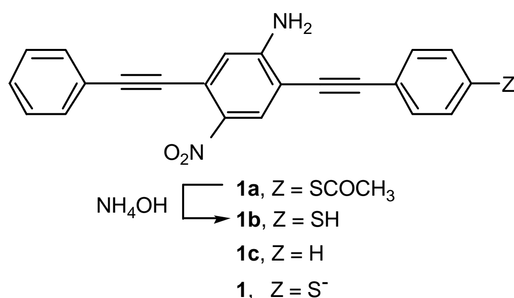

Fig. 1. The structures of active molecular compound **1**, and its precursors, the free thiol **1b** and the thiol-protected system **1a**.

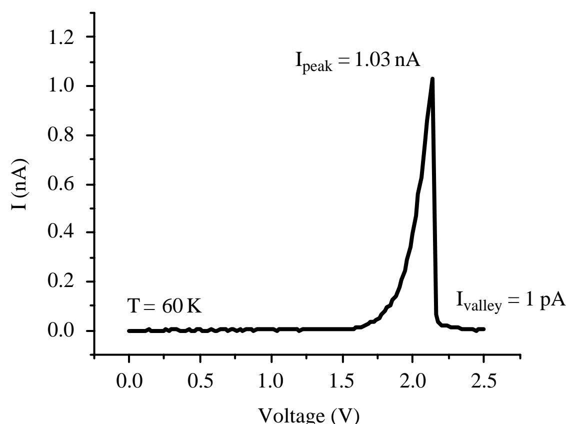

Fig. 2. $I(V)$ characteristics of a Au-**1**-Au device at 60 K. The peak current density is ~50 A/cm^2, the NDR is ~ -400 μΩ cm^2, and the PVR is 1030:1.

benzenethiolate (**1**) upon exposure to Au after 48 h [3] under an inert atmosphere of Ar.

A device containing a SAM of conjugated molecules similar to **1** but not bearing the nitroamine functionalities was fabricated and measured in nearly identical conditions and did not exhibit any NDR behavior. Therefore, the nitroamine redox center is responsible for the NDR behavior.

Typical $I(V)$ characteristics of a Au-(**1**)-Au device at 60 K are shown in Fig. 2. Positive bias corresponds to hole injection from the chemisorbed thiol-Au contact and electron injection from the evaporated contact. The peak current density for this device was greater than 53 A/cm^2, the NDR is less than -380 μΩ cm^2, and the peak-to-valley ratio (PVR) is 1030:1. Unlike previous devices that also used molecules to form the active region [4], this device exhibits a robust and large NDR. Some device-to-device variations of peak voltage position ($\sim\times 2$) and peak current ($\sim\times 4$) were observed. The $I(V)$ curve is fully reversible upon change in bias sweep direction (from negative bias to positive bias); for a given device, small fluctuations (~1% in voltage peak position and ~6% in peak current) are observed with consecutive positive and negative sweeps but could be attributed to temperature fluctuations of ~2 K (within the experimental thermal stability). The performance exceeds that observed in typical solid state quantum well resonant tunneling heterostructures [5–8]. In addition to the obvious size advantages for scaling, the intrinsic device characteristics (that is, the valley current shutoff) may be superior to that of solid state devices. The intrinsic PVR of the molecule may be considerably greater than that reported here because the valley currents observed (on the order of picoamperes) are comparable to typical leakage currents in the silicon nitride film. At negative bias, when electrons were injected from the chemisorbed contact, the current level is approximately one order of magnitude smaller than that of positive bias (Fig. 3).

All of the Au-**1c**-Au devices examined exhibit peak voltage position and current magnitude shifts with temperature such as shown in Fig. 4. We observe a decrease in peak intensity with increasing temperature. We also observe that the peak position shifts to smaller voltage with increasing temperature. The shift can be fit by the following expression:

$$\Delta V_{\text{peak}} = \frac{c_1}{1 + \mathrm{e}^{-34(\text{meV})/kT}}.$$

This expression can be explained by a two energy level model using a Boltzmann distribution, where the 34 (±0.7) meV corresponds to an activation barrier.

Modifications of the sidegroup moities were performed to observe the effect on the transport characteristics. Fig. 5 lists the molecules used in this study. The four systems studied are: Au-(**1**)-Au (**1**: 2′-amino-4, 4′-di(ethynylphenyl)-5′-nitro-1-benzenethiolate); Au-(**2**)-Au (**2**: 4, 4′-di(ethynylphenyl)-2′-nitro-1-benzenethiolate); Au-(**3**)-Au (**3**: 2′-amino-4, 4′-di(ethynylphenyl)-1-benzenethiolate); as well as Au-(**4**)-Au (**4**: 4, 4′-di(ethynylphenyl)-1-benzenethiolate) that had neither the nitro nor amine functionalities.

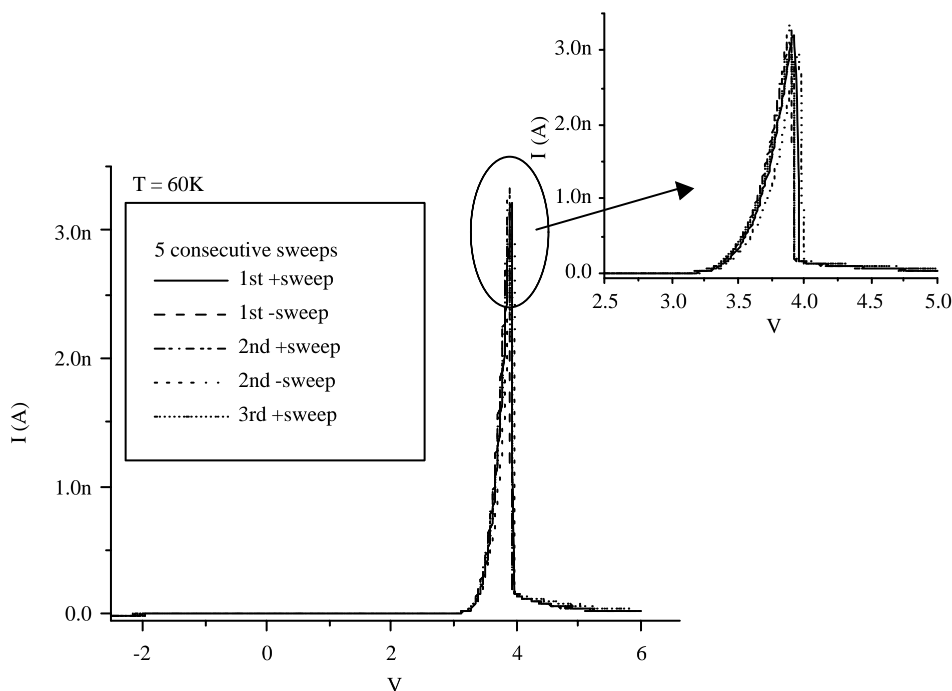

Fig. 3. Forward $(-2 \rightarrow 6)$V and reverse $(6 \rightarrow -2)$V sweeps on Au-**1c**-Au junction at 60 K. The inset shows the blowup of the sweeps around peak.

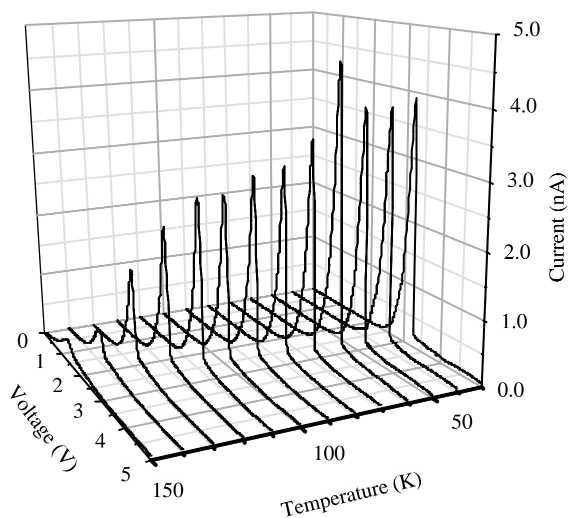

Fig. 4. $I(V,T)$ characteristics of a Au-**1c**-Au device.

Similar NDR behavior is also observed in devices with nitro only moiety (**2**). The PVR is smaller than that of **1**, but NDR behavior persisted from low temperature to room temperature. $I(V)$ characteristics of a Au-(**2**)-Au device at 300 K is shown in Fig. 6. The device has 300 K characteristics of a peak current density greater than 16 A/cm^2, NDR smaller than -144 $m\Omega\ cm^2$ and a PVR of 1.5:1. At 190 K (Fig. 6b), the NDR peak is much sharper than that of **1**, although its PVR is not as big as that of **1**. The degradation in PVR (decreasing in peak current) can probably be caused by increased inelastic scattering with increasing temperature.

The next experiment that naturally follows is the electronic transport and electrochemistry experiments of amino only molecule (2′-amino-4, 4′-di(ethynyl-phenyl)-1-benzenethiolate, compound 3). We observe no NDR behavior in 3 at both low temperature (60 K) and room temperature. Concluding from above experimental results, we suggest that the nitro group is responsible for the NDR behavior.

These SAMs also exhibit memory phenomena. Here we demonstrate nanoscale electronically programmable and erasable memory devices utilizing molecular SAM; and a memory cell applicable to a random access memory (RAM).

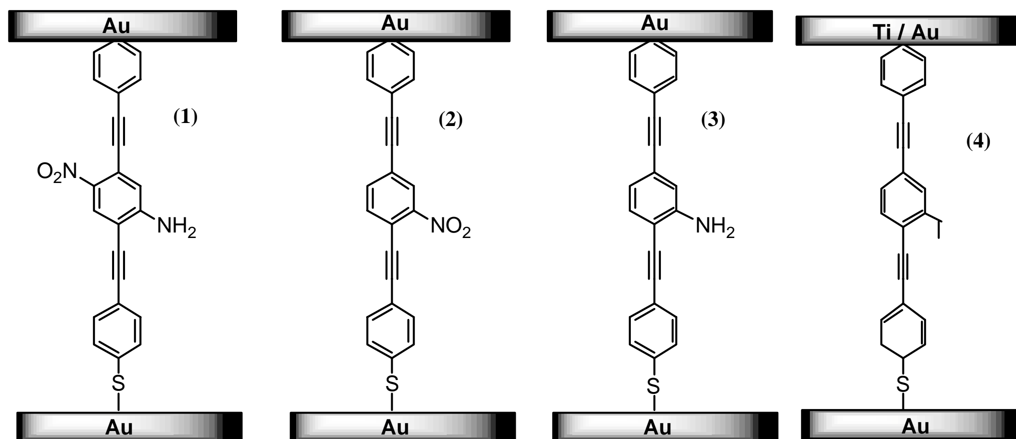

Fig. 5. The molecular junctions (**1**–**4**) used in this study. There are approximately 1000 molecules sandwiched between the two Au contacts. Only one molecule is drawn for simplicity.

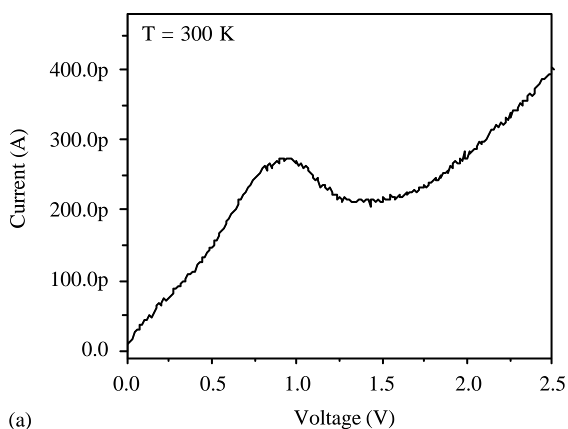

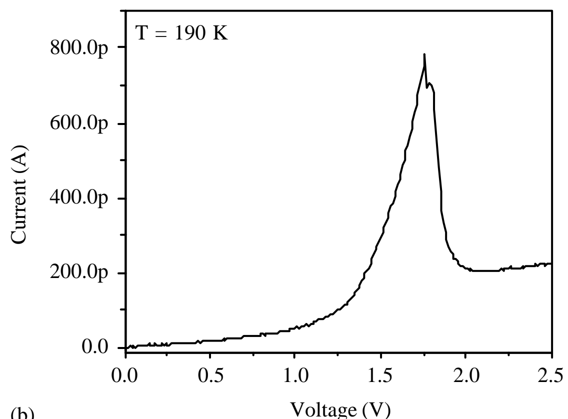

Fig. 6. $I(V)$ characteristics of a Au-**2**-Au device at (a) 300 K, (b) 190 K.

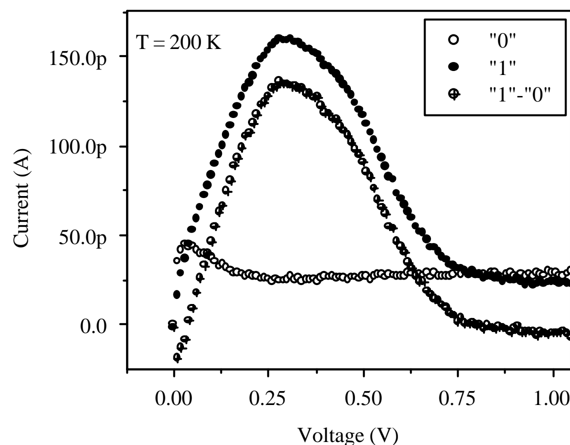

Fig. 7. $I(V)$ characteristics of a Au-(**1**)-Au device at 200 K. “0” denotes the initial state, “1” the stored written state, and “1”−“0” the difference of the two states.

The memory device operates by the storage of a high or low conductivity state upon application of a voltage pulse. The high σ state persists as a stored “bit”, which is unaffected by successive read pulses. Molecules with the nitro moieties (**1** and **2**) are observed to change conductivity state, whereas the amine only (**3**) and the unfunctionalized molecule (**4**) do not exhibit storage.

Fig. 7 shows the $I(V)$ characteristics of a Au-(**1**)-Au device at 200 K initially (defined as “0”) and after (defined as “1”) a write pulse, as well as

the difference between the two (defined as "1"−"0"). Positive bias corresponds to hole injection from the chemisorbed thiol-Au contact. The device initially probed with a positive voltage sweep from 0 to 2 V in 1 min exhibits a low conductivity state. Subsequent positive sweeps show a high conductivity state with $I(V)$ characteristics identical to the previous values ("1"). Device bias swept in the reverse bias direction from 0 to −2 V in 1 min causes the $I(V)$ to be identically reset to the initial, "0" $I(V)$ characteristic. The characteristics are repeatable to high accuracy and device degradation is not observed. This ability to program, read, and refresh the state of the molecular device accomplishes the functionality of a RAM.

A characteristic bit retention time was obtained by measuring the stored high conductivity state at various times intervals after programming the Au-(**1**)-Au device. After an initial positive write sweep from 0 to 2 V in 1 min, a second sweep was measured at different time intervals, and the difference between the first and the second sweeps at peak current position was taken and plotted against time in Fig. 8. Notice that after each second sweep during the experiment, the junction has to be reset to the initial state by a negative bias sweep from 0 to −2 V in 1 min. It is found that the difference "1"−"0" exhibits an exponential decay with a time constant (τ) of approximately 800 s at 260 K. Similar measurements were performed from 260 to 190 K. The stored state was found to decay exponentially with increasing time constants at lower temperatures. Shown in Fig. 8 is a plot of the decay time constant (retention time) at different temperatures, exhibiting an exponential dependence with $1/T$. It indicates an activation behavior: $\tau = \tau_0 \exp(E_a/kT)$, suggesting activation over a single trap state. The activation energy E_a for this molecule over this bias regime was found to be approximately 80 meV.

Memory effects are also observed in devices with the molecules having only the nitro moiety (**2**) (Memory effects are not observed in molecule (**3**) with amine-only group.), although in this case the storage was of a *low* conductivity state. $I(V)$ characteristics under negative biases are shown in Fig. 9(a). It shows the first/initial, and second sweeps from 0 to −5 V in 2 min, respectively. As described before, subsequent reads and resets identically recovered the $I(V)$ characteristics. Fig. 9(b) shows the difference $I(V)$ sweeps ("0"−"1") at various temperatures. The width of the current plateau decreases with increasing temperature, similar to that of molecule (**1**).

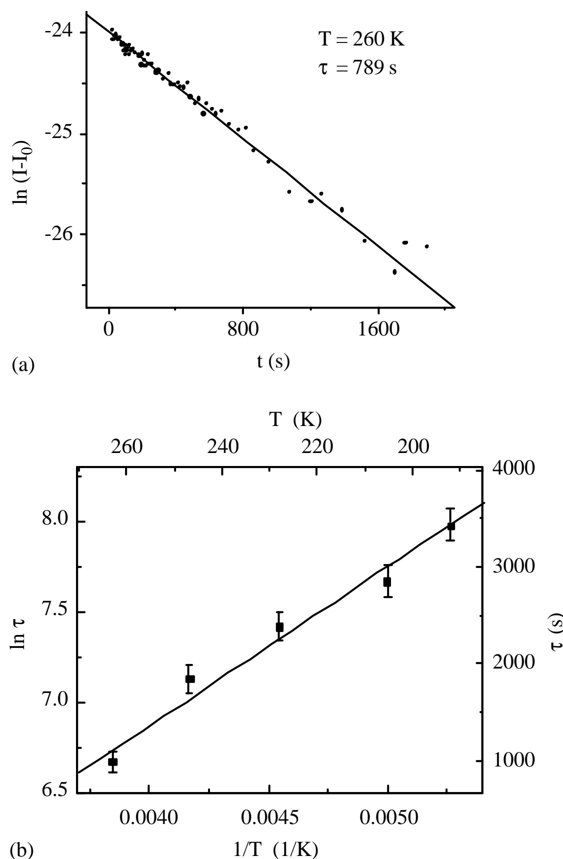

Fig. 8. Bit retention as a function of time and temperature. (a) Bit retention for (**1**) exhibits an exponential decay with a time constant (τ) of 790 s at 260 K. (b) Temperature dependence of τ gives an activation energy $E_a = 76 \pm 7$ meV.

A characteristic bit retention time is obtained by measuring the stored *low* conductivity state at various times intervals after programming the Au-(**2**)-Au device. After an initial write bias sweep, current (I_1) at 1.5 V of the stored state "1" increases gradually till it recovers the initial "0" high conductivity state (I_0). Their difference ($I_0 - I_1$) exhibits an exponential decay with a time constant (τ) of approximately 900 s at 300 K.

The storage of a persistent conductivity state in the region of a NDR peak is shown in Fig. 10. The molecule is a biphenyl-dinitro (shown in the figure), and the results are at 300 K. Note here the NDR peak essentially disappears, and can be recovered.

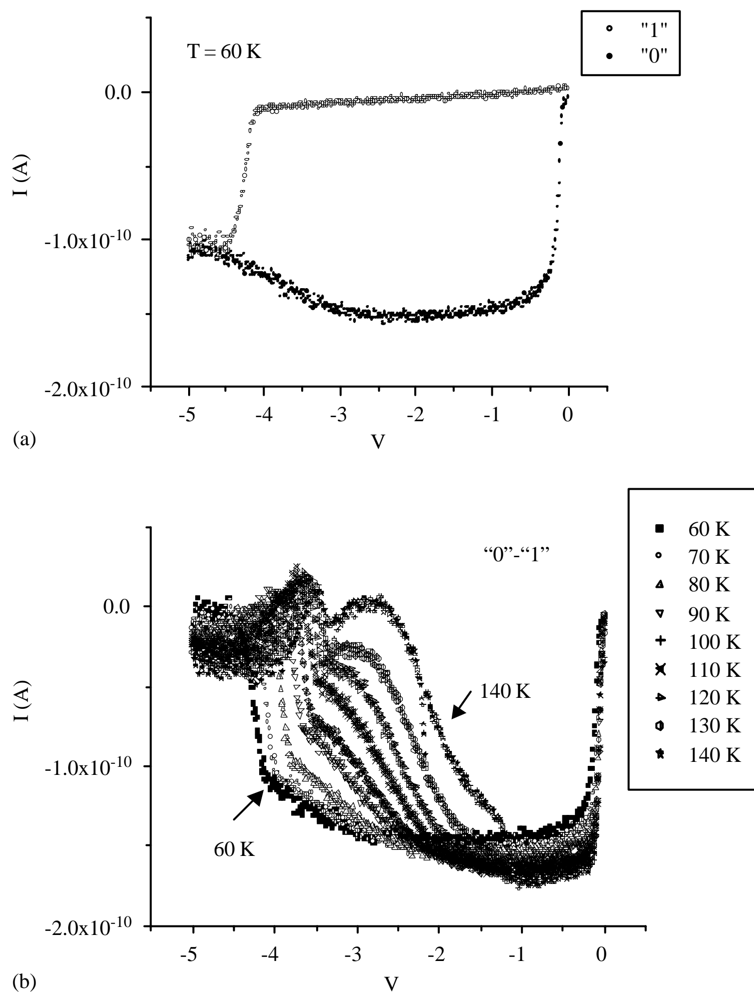

Fig. 9. (a) $I(V)$ characteristics of the first trace (initial state) and the second trace (stored state) in Au-(**2**)-Au at 60 K under negative bias; (b) difference $I(V)$ characteristics ("0"−"1") at various temperatures.

To illustrate application of this memory effect, a memory circuit was constructed utilizing a Au-**2**-Au device in combination with a sense circuit, effectively demonstrating a molecular RAM cell at ambient temperature. Fig. 11 shows the TTL-compatible I/Os of this circuit. The upper trace in Fig. 11 is an input waveform applied to the device, and the lower is the RAM cell output. The first positive pulse configures the state of the cell by writing a bit, and the second and third positive pulses read the cell. The third pulse (and subsequent read pulses, not shown here for simplicity) demonstrates that the cell is robust and continues to hold the state (up to the limit of the bit retention time. This demonstration highlights the dramatically long bit retention time). The negative pulse erases the bit, resetting the cell. The second set of 4 pulses repeats this pattern, and many hours of continuous operation have been observed with no degradation in performance. Currently, the speed of the memory device is limited by the RC time constant of the circuit. The current level of the devices is less than 10 nA, which can be attributed to the 0.7 eV S-Au barrier in the molecular junction. Engineering of molecules with smaller contact barriers (e.g., use CN terminated molecules and Pd contacts) to obtain higher current level while minimizing contact area to

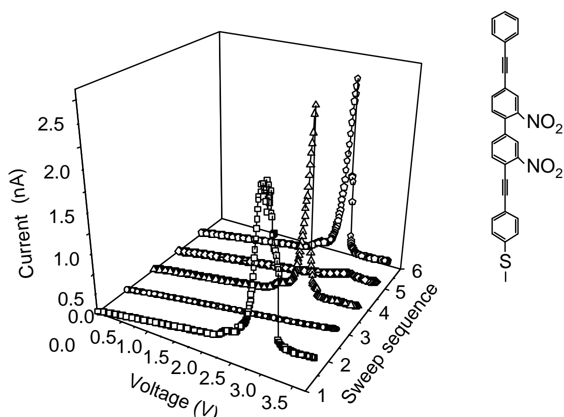

Fig. 10. *I–V* characteristics of a Au-biphenyl dinitro-Au device. 1st sweep shows high conductivity ON-state and two NDR peaks, the prominent peak current is 2.5 nA, the PVR is 7:1. The subsequent sweeps show low conductivity OFF-state. After a negative sweep, the high conductivity ON-state recovered and repeated with the 1st sweep. The subsequent sweeps show same low conductivity. After a negative sweep, the high conductivity ON-state recovers.

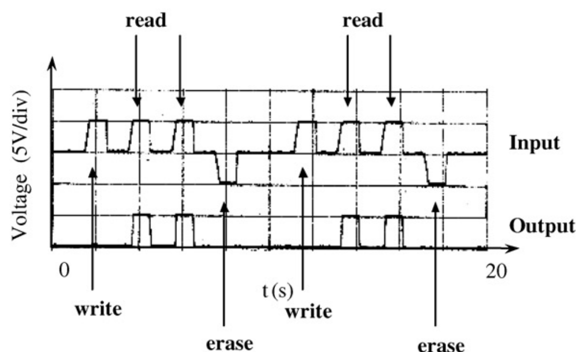

Fig. 11. Measured logic diagram of the molecular random access memory.

decrease parasitic capacitance should improve the RC limit.

The present devices utilize nanoscale structures that limit the number of molecules in the active region to ~1000, which is determined by lithographic limitations in defining the contacts. We have seen no evidences in the device characteristics indicating that limitations exist for scaling the number of molecules in the active region to one, assuming that an appropriate fabrication scheme can be identified.

We demonstrated novel non-FET switching devices and a prototype memory cell using single SAMs as the active component. We have realized two-terminal NDR devices with large PVR at low temperature and NDR devices at room temperature. Based on our experiments, the electron-withdrawing nitro group is responsible for NDR behavior, whereas the electron-donating amine group gives rise to a bound state in the molecule of approximately 30 meV. We also discovered erasable storage effects in redox-center-containing ethynylphenyl molecules. The storage behavior can be discreetly added on a molecule by engineering electron-withdrawing or/and electron-donating sidegroups onto its backbone. Finally, we successfully demonstrated an erasable molecular memory cell that can store a high conductivity state with a bit retention time orders of magnitudes longer than that of a DRAM.

References

[1] R.S. Potember, T.O. Pochler, D.O. Cowan, Appl. Phys. Lett. 34 (1979) 405–407.

[2] R.S. Potember, T.O. Poehler, D.O. Cowan, A.N. Bloch, Electrical switching and memory phenomena in semiconducting organic charge-transfer complexes, in: L. Alcbcer (Ed.), The Physics and Chemistry of Low-dimensional Solids, Reidel, Dordrecht, 1980, pp. 419–428.

[3] J.M. Tour, et al., J. Am. Chem. Soc. 117 (1995) 9529.

[4] M.A. Reed, Proc. IEEE 87 (1999) 652.

[5] J.H. Smet, T.P.E. Broekaert, C.G. Fonstad, J. Appl. Phys. 71 (1992) 2475.

[6] J.R. Söderström, D.H. Chow, T.C. McGill, J. Appl. Phys. 66 (1989) 5106.

[7] J. Day, et al., J. Appl. Phys. 73 (1993) 1542.

[8] H.H. Tsai, et al., IEEE Elec. Dec. Lett. 15 (1993) 357.